The Astrophysical Journal, 733:66 (9pp), 2011 May 20 doi:10.1088/0004-637X/733/1/66

CONTRIBUTION OF GAMMA-RAY-LOUD RADIO GALAXIES' CORE EMISSIONS TO THE COSMIC MeV AND GeV GAMMA-RAY BACKGROUND RADIATION

Yoshiyuki Inoue[1,2]
[1] Department of Astronomy, Kyoto University, Kitashirakawa, Sakyo-ku, Kyoto 606-8502, Japan; yinoue@kusastro.kyoto-u.ac.jp
[2] Max Planck Institute for Physics, Föhringer Ring 6, 80805 Munich, Germany
Received 2010 December 29; accepted 2011 March 20; published 2011 May 5

ABSTRACT

The *Fermi* gamma-ray satellite has recently detected gamma-ray emissions from radio galaxy cores. From these samples, we first examine the correlation between the luminosities at 5 GHz, $L_{5\,\mathrm{GHz}}$, and at 0.1–10 GeV, L_γ, of gamma-ray-loud radio galaxies. We find that the correlation is significant with $L_\gamma \propto L_{5\,\mathrm{GHz}}^{1.16}$ based on a partial correlation analysis. Using this correlation and the radio luminosity function (RLF) of radio galaxies, we explore the contribution of gamma-ray-loud radio galaxies to the unresolved extragalactic gamma-ray background (EGRB). The gamma-ray luminosity function is obtained by normalizing the RLF to reproduce the source-count distribution of the *Fermi* gamma-ray-loud radio galaxies. We find that gamma-ray-loud radio galaxies can explain ∼25% of the unresolved *Fermi* EGRB flux above 100 MeV and will also make a significant contribution to the EGRB in the 1–30 MeV energy band. Since blazars explain 22% of the EGRB above 100 MeV, radio-loud active galactic nucleus populations explain ∼47% of the unresolved EGRB. We further make an interpretation on the origin of the EGRB. The observed EGRB spectrum at 0.2–100 GeV does not show an absorption signature by the extragalactic background light. Thus, the dominant population of the origin of EGRB at very high energy (>30 GeV) might be either nearby gamma-ray-emitting sources or sources with very hard gamma-ray spectra.

Key words: diffuse radiation – galaxies: active – gamma rays: diffuse background

Online-only material: color figures

1. INTRODUCTION

The origin of the extragalactic diffuse MeV and GeV gamma-ray background (EGRB) radiation has been debated for a long time in astrophysics, although it is well known that radio-quiet active galactic nuclei (AGNs) take into account the cosmic X-ray background (CXB) below several hundred keV (see, for reviews, Boldt 1987; Fabian & Barcons 1992; Ueda et al. 2003; Hasinger et al. 2005; Gilli et al. 2007). The EGRB spectrum at 0.3–30 MeV is measured by the *Solar Maximum Mission* (*SMM*; Watanabe et al. 1997) and the Imaging Compton Telescope (COMPTEL) on board the *Compton Gamma-Ray Observatory* (*CGRO*; Kappadath et al. 1996). EGRB was first discovered in the GeV energy range by the satellite *Small Astronomy Satellite-2* (*SAS-2*; Fichtel et al. 1978; Thompson & Fichtel 1982). Energetic Gamma-Ray Experiment Telescope (EGRET) on board the *CGRO* confirmed the EGRB spectrum at 0.03–50 GeV (Sreekumar et al. 1998; Strong et al. 2004). Recently, the Large Area Telescope (LAT) on board the *Fermi Gamma-Ray Space Telescope* (*Fermi*) made a new measurement of the EGRB spectrum from 0.2 to 100 GeV (Abdo et al. 2010e). The observed integrated EGRB flux ($E > 100$ MeV) is 1.03×10^{-5} photons cm^{-2} s^{-1} sr^{-1} with a photon index of 2.41.

Several sources have been suggested to explain the MeV background. One is the nuclear decay gamma-ray from Type Ia supernovae (SNe Ia; Clayton & Ward 1975; Zdziarski 1996; Watanabe et al. 1999). However, the recent measurement of the cosmic SNe Ia rate suggests that the expected flux from SNe Ia is one order of magnitude lower than the measured MeV EGRB flux (Ahn et al. 2005; Strigari et al. 2005; Horiuchi & Beacom 2010). Comptonization emission from non-thermal electrons in AGN coronae is also proposed (Inoue et al. 2008). This model explains the origin of CXB and the MeV EGRB in the same population. Blazars, which are one type of AGN with the direction of a relativistic jet coinciding with our line of sight, are also proposed (Ajello et al. 2009). Very recently, Massaro & Ajello (2011) have shown that the gamma-ray emission from lobes of radio galaxies will explain ∼10% of the MeV background flux. MeV mass-scale dark matter (DM) annihilations have also been discussed (Ahn & Komatsu 2005a, 2005b), but there is no natural particle-physics candidate for a DM with a mass scale of MeV energies. However, discussion of the origin of the MeV background still continues due to the difficulties of making MeV gamma-ray measurements.

In the case of the GeV background, since blazars are dominant extragalactic gamma-ray sources (Hartman et al. 1999; Abdo et al. 2010g), it is expected that an unresolved population of blazars would explain the GeV EGRB (Padovani et al. 1993; Stecker et al. 1993; Salamon & Stecker 1994; Chiang et al. 1995; Stecker & Salamon 1996; Chiang & Mukherjee 1998; Mukherjee & Chiang 1999; Mücke & Pohl 2000; Narumoto & Totani 2006; Giommi et al. 2006; Dermer 2007; Pavlidou & Venters 2008; Kneiske & Mannheim 2008; Bhattacharya et al. 2009; Inoue & Totani 2009). Recently, Abdo et al. (2010f) showed that unresolved blazars can explain ∼22% of the EGRB above 0.1 GeV by analyzing the 11 month *Fermi* AGN catalog. Very recently, Stecker & Venters (2010) proposed that the unresolved blazar population would be able to explain the EGRB spectrum below 1 GeV, by taking into account the energy dependence of source-confusion effects.

Other gamma-ray-emitting extragalactic sources have also been discussed as the origin of the GeV EGRB. These are intergalactic shocks produced by the large-scale structure formation (Loeb & Waxman 2000; Totani & Kitayama 2000; Miniati 2002; Keshet et al. 2003; Gabici & Blasi 2003), normal and starburst galaxies (Pavlidou & Fields 2002; Thompson et al. 2007; Bhattacharya & Sreekumar 2009; Makiya et al. 2011; Fields et al. 2010), high Galactic latitude pulsars (Faucher-Giguère &

Table 1
Observed Parameters of Gamma-ray-loud Radio Galaxies

Object Name	1FGL Name	z	F_γ ($\times 10^{-9}$ photons cm^{-2} s^{-1})	Γ	S_R (Jy)	α_r	Class	Ref.
3C 78/NGC 1218	1FGLJ 0308.3+0403	0.029	4.7 ± 1.8	1.95 ± 0.14	0.964 ± 0.048	0.64	FRI	1
3C 84/NGC 1275	1FGLJ 0319.7+4130	0.018	222 ± 8	2.13 ± 0.02	3.10 ± 0.02	0.78	FRI	2
3C 111	1FGLJ 0419.0+3811	0.049	40 ± 8	2.54 ± 0.19	1.14 ± 0.0[a]	−0.146	FRII	3
PKS 0625-354	1FGLJ 0627.3−3530	0.055	4.8 ± 1.1	2.06 ± 0.16	0.60 ± 0.03	0.53	FRI	1
3C 207	1FGLJ 0840.8+1310	0.681	24 ± 4	2.42 ± 0.10	0.51 ± 0.02	0.9	FRII	2
PKS 0943-76	1FGLJ 0940.2−7605	0.27	55 ± 12	2.83 ± 0.16	0.79 ± 0.03	0.79	FRII	4
M87/3C 274	1FGLJ 1230.8+1223	0.004	24 ± 6	2.21 ± 0.14	4.0 ± 0.04	0.79	FRI	2
Cen A	1FGLJ 1325.6−4300	0.0009	214 ± 12	2.75 ± 0.04	6.98 ± 0.21	1.2	FRI	1
NGC 6251	1FGLJ 1635.4+8228	0.024	36 ± 8	2.52 ± 0.12	0.35 ± 0.045	0.72	FRI	2
3C 380	1FGLJ 1829.8+4845	0.0692	31 ± 18	2.51 ± 0.30	7.45 ± 0.047	0.71	FRII	2

Notes. 1FGL Name: the First Source Catalog (1FGL) *Fermi*-LAT source name, z: redshift of the source, F_γ: gamma-ray photon flux above 100 MeV in 10^{-9} photons cm^{-2} s^{-1}, Γ: photon index at 0.1–10 GeV, S_R: radio flux density at 5 GHz in Jy, α_r: radio spectral index at 5 GHz, and Class: FRI is type I of the Fanaroff–Riley galaxy and FRII is type II of the Fanaroff–Riley galaxy (Fanaroff & Riley 1974).
References. (1) Unger et al. 1984; Saikia et al. 1986; Baum et al. 1988; Ekers et al. 1989; Jones & McAdam 1992; Burns et al. 1983; Morganti et al. 1993; (2) Bennett 1962; Spinrad et al. 1985; Laing et al. 1983; (3) Linfield & Perley 1984; (4) Burgess & Hunstead 2006a, 2006b.
[a] No error is reported in Linfield & Perley (1984).

Loeb 2010; Siegal-Gaskins et al. 2010), kiloparsec (kpc)-size AGN jets (Stawarz et al. 2006), radio-quiet AGNs (Inoue et al. 2008; Inoue & Totani 2009), and GeV mass-scale DM annihilation or decay (see, e.g., Jungman et al. 1996; Bergström 2000; Ullio et al. 2002; Oda et al. 2005; Ando & Komatsu 2006; Horiuchi & Ando 2006; Ando et al. 2007; Ahn et al. 2007; Ando 2009; Kawasaki et al. 2009).

Fermi has recently detected GeV gamma-ray emissions from 11 misaligned AGNs (i.e., radio galaxies), which are one type of AGN with the direction of a relativistic jet *not* coinciding with our line of sight (Abdo et al. 2010b). Their average photon index at 0.1–10 GeV is ∼2.4, which is the same as that of the GeV EGRB (Abdo et al. 2010e) and blazars (Abdo et al. 2010f). Although they are fainter than blazars, the expected number in the entire sky is much higher than the number of blazars. It is naturally expected, then, that they will make a significant contribution to the EGRB. Therefore, in this paper, we study the contribution of such gamma-ray-loud radio galaxies (not blazars) to the EGRB.

To study the contribution of gamma-ray-loud radio galaxies to the EGRB, their gamma-ray luminosity function (GLF) is required. Because samples are limited, it is not straightforward to construct it using only *Fermi* samples. Therefore, we first investigate the correlation between radio and gamma-ray luminosities of gamma-ray-loud radio galaxies. In the case of blazars, the correlation between gamma-ray and radio luminosities has been presented in many papers since the EGRET era (Padovani et al. 1993; Stecker et al. 1993; Salamon & Stecker 1994; Dondi & Ghisellini 1995; Zhang et al. 2001; Narumoto & Totani 2006; Ghirlanda et al. 2010, 2011). Since the radio luminosity function (RLF) of radio galaxies is well studied (see, e.g., Dunlop & Peacock 1990; Willott et al. 2001), we are able to obtain the GLF by converting it from the RLF using a luminosity correlation. With this GLF, we evaluate their contribution to the EGRB.

This work is organized as follows. Samples used in this study are shown in Section 2. In Section 3, we will investigate the radio and gamma-ray luminosity correlation and determine the GLF to reproduce the number of detected gamma-ray-loud radio galaxies. We then calculate the EGRB and compare it with the observed data in Section 4. In Section 5, we discuss the results, and give our conclusion in the sixth and final section. Throughout this paper, we adopt the standard cosmological parameters of $(h, \Omega_M, \Omega_\Lambda) = (0.7, 0.3, 0.7)$.

2. SAMPLES

During a 15-month survey of the entire sky *Fermi* reported the detection of 11 Fanaroff–Riley (FR) radio galaxies consisting of 7 type-I FR (FRI) galaxies and 4 type-II FR (FRII) galaxies. (Abdo et al. 2010b). FRI galaxies have decelerating jets, knots at a distance from the core of 1 kpc, and edge-darkened lobes, while FRII galaxies have relativistic jets and edge-brightened radio lobes with bright hotspots (Fanaroff & Riley 1974). In the AGN jet unification scenario, FRI and FRII galaxies are the misaligned AGN populations of BL Lac objects and flat spectrum radio quasars (FSRQs), respectively (Urry & Padovani 1995).

In this study, we use 10 samples (6 FRIs and 4 FRIIs) from Abdo et al. (2010b), which were already reported in the 11 month *Fermi* catalog (Abdo et al. 2010a, 2010g). This is because, as discussed in Section 3, we use the detection efficiency of *Fermi* shown in Abdo et al. (2010f) which is constructed from the 11 month catalog. Table 1 lists the gamma-ray-loud radio galaxy samples used in this study. It gives the object name, the First Source Catalog (1FGL) *Fermi*-LAT source name, redshift, gamma-ray photon flux above 0.1 GeV, photon index at 0.1–10 GeV, radio flux at 5 GHz, spectral index at 5 GHz, and radio classification. The photon index, Γ, and the spectral index, α, are the index of the power-law differential photon spectrum, $dN/d\epsilon \propto \epsilon^{-\Gamma}$ and $\Gamma - 1$, respectively.

From Table 1, the mean photon index of gamma-ray spectra at 0.1–10 GeV, Γ_c, is 2.39 and the spread is 0.28. This index is same as that of blazars, 2.40 (Abdo et al. 2010f), and the EGRB spectrum, 2.41 (Abdo et al. 2010e).

From individual source studies (Abdo et al. 2009b, 2009c, 2010c), the typical gamma-ray spectral energy distributions (SEDs) are well explained by synchrotron-self-Compton emission models. Here, by taking into account the particle cooling effect, the electron spectrum is given by $dN/d\gamma_e \propto \gamma_e^{-p}$ at $\gamma_e \leqslant \gamma_{\rm br}$ and $dN/d\gamma_e \propto \gamma_e^{-(p+1)}$ at $\gamma_e > \gamma_{\rm br}$, where $\gamma_{\rm br}$ is the cooling break Lorentz factor. The inverse Compton (IC) photon

spectrum is given by

$$dN/d\epsilon \propto \begin{cases} \epsilon^{-(p+1)/2} & \epsilon \leqslant \epsilon_{\rm br}, \\ \epsilon^{-(p+2)/2} & \epsilon > \epsilon_{\rm br}, \end{cases} \quad (1)$$

where $\epsilon_{\rm br}$ corresponds to the IC photon energy from electrons with $\gamma_{\rm br}$ (Rybicki & Lightman 1979).

The SED fitting for NGC 1275 and M87 shows that the IC peak energy in the rest frame is located at ∼5 MeV (Abdo et al. 2009b, 2009c). In this study, we use the mean photon index, Γ_c, as Γ at 0.1–10 GeV and set a peak energy, $\epsilon_{\rm br}$, in the photon spectrum at 5 MeV for all gamma-ray-loud radio galaxies as a baseline model. Then, we are able to define the average SED shape of gamma-ray-loud radio galaxies for all luminosities as $dN/d\epsilon \propto \epsilon^{-2.39}$ at $\epsilon > 5$ MeV and $dN/d\epsilon \propto \epsilon^{-1.89}$ at $\epsilon \leqslant 5$ MeV by following Equation (1).

However, only three sources are currently studied with multi-wavelength observational data. We need to make further studies of individual gamma-ray-loud radio galaxies to understand their SED properties in wide luminosity ranges. We examine other spectral models in Section 5.2.

3. GAMMA-RAY LUMINOSITY FUNCTION

3.1. Radio and Gamma-ray Luminosity Correlation

To estimate the contribution of gamma-ray-loud radio galaxies to the EGRB, we need to construct a GLF. However, because of the small sample size, it is difficult to construct a GLF using current gamma-ray data alone. Here, the RLF of radio galaxies has been extensively studied in previous works (see, e.g., Dunlop & Peacock 1990; Willott et al. 2001). If there is a correlation between the radio and gamma-ray luminosities, we are able to convert the RLF to the GLF with that correlation. In the case of blazars, it has been suggested that there is a correlation between the radio and gamma-ray luminosities from the EGRET era (Padovani et al. 1993; Stecker et al. 1993; Salamon & Stecker 1994; Dondi & Ghisellini 1995; Zhang et al. 2001; Narumoto & Totani 2006), although it has also been discussed that this correlation cannot be firmly established because of flux-limited samples (Muecke et al. 1997). Recently, using the *Fermi* samples, Ghirlanda et al. (2010, 2011) confirmed that there is a correlation between the radio and gamma-ray luminosities.

To examine a luminosity correlation in gamma-ray-loud radio galaxies, we first derive the radio and gamma-ray luminosity of gamma-ray-loud radio galaxies as follows. Gamma-ray luminosities between the energies ϵ_1 and ϵ_2 are calculated by

$$L_\gamma(\epsilon_1, \epsilon_2) = 4\pi d_L(z)^2 \frac{S_\gamma(\epsilon_1, \epsilon_2)}{(1+z)^{2-\Gamma}}, \quad (2)$$

where $d_L(z)$ is the luminosity distance at redshift, z, Γ is the photon index, and $S(\epsilon_1, \epsilon_2)$ is the observed energy flux between the energies ϵ_1 and ϵ_2. The energy flux is given from the photon flux F_γ, which is in the unit of photons cm^{-2} s^{-1}, above ϵ_1 by

$$S_\gamma(\epsilon_1, \epsilon_2) = \frac{(\Gamma-1)\epsilon_1}{\Gamma-2}\left[\left(\frac{\epsilon_2}{\epsilon_1}\right)^{2-\Gamma} - 1\right] F_\gamma, \ (\Gamma \neq 2) \quad (3)$$

$$S_\gamma(\epsilon_1, \epsilon_2) = \epsilon_1 \ln(\epsilon_2/\epsilon_1) F_\gamma, \quad (\Gamma = 2). \quad (4)$$

Radio luminosity is calculated in the same manner.

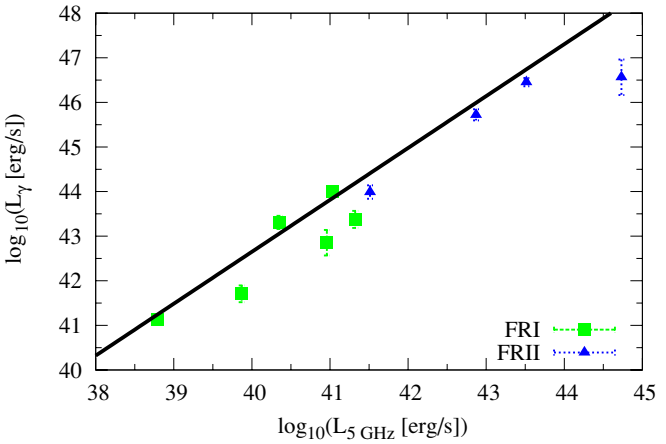

Figure 1. Gamma-ray luminosity at 0.1–10 GeV vs. radio luminosity at 5 GHz. The square and triangle data represent FRI and FRII galaxies, respectively. The solid line is the fit to all sources.

(A color version of this figure is available in the online journal.)

Figure 1 shows the 5 GHz and 0.1–10 GeV luminosity relation of *Fermi* gamma-ray-loud radio galaxies. Square and triangle data represent FRI and FRII radio galaxies, respectively. The solid line shows the fitting line to all the data. The function is given by

$$\log_{10}(L_\gamma) = (-3.90 \pm 0.61) + (1.16 \pm 0.02) \log_{10}(L_{5\,\rm GHz}), \quad (5)$$

where errors show 1σ uncertainties. In the case of blazars, the slope of the correlation between $L_\gamma(>100\,\rm MeV)$, luminosity above 100 MeV, and radio luminosity at 20 GHz is 1.07 ± 0.05 (Ghirlanda et al. 2011). The correlation slopes of gamma-ray-loud radio galaxies are similar to those of blazars. This indicates that the emission mechanism is similar in gamma-ray-loud radio galaxies and blazars.

We need to examine whether the correlation between the radio and gamma-ray luminosities is true or not. In the flux-limited observations, the luminosities of samples are strongly correlated with redshifts. This might result in a spurious luminosity correlation. As in previous works on blazar samples (Padovani 1992; Zhang et al. 2001; Ghirlanda et al. 2011), we perform a partial correlation analysis to test the correlation between the radio and gamma-ray luminosities excluding the redshift dependence (see the Appendix for details). First, we calculate the Spearman rank–order correlation coefficients (see, e.g., Press et al. 1992). The correlation coefficients are 0.993, 0.993, and 0.979 between $\log_{10} L_{5\,\rm GHz}$ and $\log_{10} L_\gamma$, between $\log_{10} L_{5\,\rm GHz}$ and redshift, and between $\log_{10} L_\gamma$ and redshift, respectively. Then, the partial correlation coefficient becomes 0.866 with chance probability 1.65×10^{-6}. Therefore, we conclude that there is a correlation between the radio and gamma-ray luminosities of gamma-ray-loud radio galaxies.

3.2. Gamma-ray Luminosity Function

In this section, we derive the GLF of gamma-ray-loud radio galaxies, $\rho_\gamma(L_\gamma, z)$. There is a correlation between the radio and gamma-ray luminosities as shown in Equation (5). With this correlation, we develop the GLF by using the RLF of radio galaxies, $\rho_r(L_r, z)$, with radio luminosity, L_r. The GLF is given

Table 2
The Parameters of the RLF

RLF Model	Willott et al. (2001)
$\log_{10}(\rho_{\rm I,0}{}^{\rm a})$	−7.523
$\alpha_{\rm I}$	0.586
$\log_{10}(L_{\rm I,c}{}^{\rm b})$	26.48
$z_{\rm I,c}$	0.710
$k_{\rm I}$	3.48
$\log_{10}(\rho_{\rm II,0}{}^{\rm a})$	−6.757
$\alpha_{\rm II}$	2.42
$log_{10}(L_{\rm II,c}{}^{\rm b})$	27.39
$z_{\rm II,c}$	2.03
$z_{\rm II,1}$	0.568
$z_{\rm II,2}$	0.956

Notes.
[a] In units of $\rm Mpc^{-3}$.
[b] In units of $\rm W\,Hz^{-1}\,sr^{-1}$.

as

$$\rho_\gamma(L_\gamma, z) = \kappa \frac{dL_r}{dL_\gamma}\rho_r(L_r, z), \quad (6)$$

where κ is a normalization factor. We use the 151 MHz RLF (Willott et al. 2001). Since Willott et al. (2001) presented the formulas of FRI and FRII RLFs separately, we combined them as in their paper, because it is difficult to analyze each population separately using our limited number of samples. Moreover, since the cosmological parameters in Willott et al. (2001) are $\Omega_M = \Omega_\Lambda = 0$ and $h = 0.5$, we also convert the RLF to the standard cosmology adopted in this study. The RLF is given by

$$\rho_r(L_r, z) = \eta(z) \times [\rho_{r,\rm FRI}(L_r, z) + \rho_{r,\rm FRII}(L_r, z)], \quad (7)$$

where $\eta(z)$ is the conversion factor of cosmology, $\rho_{r,\rm FRI}$ is the FRI RLF, and $\rho_{r,\rm FRII}$ is the FRII RLF. The FRI RLF and FRII RLF are given by

$$\rho_{r,\rm FRI}(L_r, z) = \begin{cases} \rho_{\rm I,0}\left(\frac{L_r}{L_{\rm I,c}}\right)^{-\alpha_{\rm I}} \exp\left(\frac{-L_r}{L_{\rm I,c}}\right)(1+z)^{k_{\rm I}} & z \leqslant z_{\rm I,c}, \\ \rho_{\rm I,0}\left(\frac{L_r}{L_{\rm I,c}}\right)^{-\alpha_{\rm I}} \exp\left(\frac{-L_r}{L_{\rm I,c}}\right)(1+z_{\rm I,c})^{k_{\rm I}} & z > z_{\rm I,c}, \end{cases} \quad (8)$$

$$\rho_{r,\rm FRII}(L_r, z) = \rho_{\rm II,0}\left(\frac{L_r}{L_{\rm II,c}}\right)^{-\alpha_{\rm II}} \exp\left(\frac{-L_{\rm II,c}}{L_r}\right) f_{\rm II}(z). \quad (9)$$

Here, $f_{\rm II}(z)$ is the evolution function given by

$$f_{\rm II}(z) = \begin{cases} \exp\left[-\frac{1}{2}\left(\frac{z-z_{\rm II,c}}{z_{\rm II,1}}\right)\right] & z \leqslant z_{\rm II,c}, \\ \exp\left[-\frac{1}{2}\left(\frac{z-z_{\rm II,c}}{z_{\rm II,2}}\right)\right] & z > z_{\rm II,c}. \end{cases} \quad (10)$$

The parameters of these RLFs are summarized in Table 2. As in Stawarz et al. (2006), the conversion factor of the cosmology $\eta(z)$ is

$$\eta(z) \equiv \frac{d^2V_W/d\Omega dz}{d^2V/d\Omega dz}. \quad (11)$$

The comoving volume element of cosmology in Willott et al. (2001) is

$$\frac{d^2V_W}{d\Omega dz} = \frac{c^3z^2(2+z)^2}{4H_{0,W}^3(1+z)^3}, \quad (12)$$

where c is the speed of light and $H_{0,W}$ is $50\,\rm km\,s^{-1}\,Mpc^{-1}$. The comoving volume element of our standard cosmology is

$$\frac{d^2V}{d\Omega dz} = \frac{cd_L(z)^2}{H_0(1+z)^2\sqrt{(1-\Omega_M-\Omega_\Lambda)(1+z)^2+\Omega_M(1+z)^3+\Omega_\Lambda}}, \quad (13)$$

where H_0 is $70\,\rm km\,s^{-1}\,Mpc^{-1}$.

Since Equation (5) is for radio luminosities at 5 GHz in the unit of erg $\rm s^{-1}$, we assume spectral index $\alpha_r = 0.8$ for all radio galaxies to convert 151 MHz luminosity to 5 GHz luminosity, as assumed in Willott et al. (2001). Although α_r would affect the fraction of gamma-ray-loud radio galaxies in the radio galaxy population, α_r does not affect the main results of the EGRB calculation in this paper because our GLF is normalized to the cumulative source-count distribution of the gamma-ray-loud radio galaxies detected by *Fermi*.

3.3. Source-count Distribution

The normalization factor κ, which corresponds to the fraction of gamma-ray-loud radio galaxies against all radio galaxies, is determined by normalizing our GLF to the source-count distribution of the *Fermi* radio galaxies, which is sometimes called $\log N$–$\log S$ plot or cumulative flux distribution. The source-count distribution is calculated by

$$N(>F_\gamma) = 4\pi \int_0^{z_{\rm max}} dz \frac{d^2V}{d\Omega dz} \int_{L_\gamma(z,F_\gamma)}^{L_{\gamma,\rm max}} dL_\gamma \rho_\gamma(L_\gamma, z), \quad (14)$$

where $L_\gamma(z, F_\gamma)$ is the gamma-ray luminosity of a blazar at redshift z whose photon flux at >100 MeV is F_γ. Hereafter, we assume $z_{\rm max} = 5$ and $L_{\gamma,\rm max} = 10^{48}\,\rm erg\,s^{-1}$ in this study. These assumptions hardly affect the results in this study.

Since the completeness of the *Fermi* sky survey depends on the photon flux and photon index of a source, we need to take into account this effect (the so-called detection efficiency) to compare the GLF with the cumulative source-count distribution of gamma-ray-loud radio galaxies. The detection efficiency of *Fermi* is shown in Figure 7 of Abdo et al. (2010f) for the sources in the 11 month catalog with test statistics TS > 50, at the Galactic latitude $|b| > 20^\circ$, and with a mean photon index of 2.40, which is similar to that of gamma-ray-loud radio galaxies (see Section 2). It is shown that the results for blazar source-count distribution analysis does not change even if samples with $|b| > 15^\circ$ are included. Furthermore, even if they include samples with TS > 25, the systematic uncertainties are small. Therefore, we adopt the detection efficiency shown in Abdo et al. (2010f) in our samples from the *Fermi* 11 month catalog, although not all the samples are located at $|b| > 20^\circ$ or have TS > 50.

Figure 2 shows the source-count distribution of gamma-ray-loud radio galaxies. The data shown are after the conversion of the detection efficiency. The solid line represents the case of $\kappa = 1$, which shows that all radio galaxies emit gamma rays. The dashed curve corresponds to the GLF fitted to the *Fermi* data with $\kappa = 0.081 \pm 0.011$. About 1000 gamma-ray-loud radio galaxies are expected during a survey of the entire sky above the flux threshold $F_\gamma(>100\,\rm MeV) = 1.0 \times 10^{-9}$ photons $\rm cm^{-2}\,s^{-1}$ above 100 MeV. We note that the current detection efficiency of *Fermi* at $F_\gamma(>100\,\rm MeV) = 1.0 \times 10^{-9}$ photons $\rm cm^{-2}\,s^{-1}$ is $\sim 10^{-3}$.

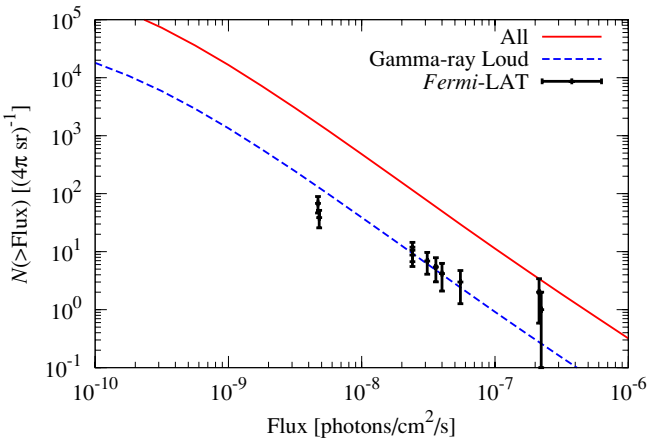

Figure 2. Source-count distribution of gamma-ray-loud radio galaxies in the entire sky. Solid and dashed curves correspond to all radio galaxies and gamma-ray-loud radio galaxies, respectively. The data points show the *Fermi* data after the conversion of the detection efficiency. The error bar shows 1σ statistical uncertainty.

(A color version of this figure is available in the online journal.)

4. EXTRAGALACTIC GAMMA-RAY BACKGROUND

We calculate the EGRB spectrum by integrating our GLF in the redshift and luminosity space, using the SED model shown in Section 2. The EGRB spectrum is calculated as

$$\frac{d^2F(\epsilon)}{d\epsilon d\Omega} = \frac{c}{4\pi}\int_0^{z_{\rm max}} dz \left|\frac{dt}{dz}\right| \int_{L_{\gamma,\rm min}}^{L_{\gamma,\rm max}} dL_\gamma \rho_\gamma(L_\gamma, z) \times \frac{dL[L_\gamma, (1+z)\epsilon]}{d\epsilon} \times \{1.0 - \omega(F_\gamma[L_\gamma, z])\} \times \exp[-\tau_{\gamma,\gamma}(\epsilon, z)], \quad (15)$$

where t is the cosmic time and dt/dz can be calculated by the Friedmann equation in the standard cosmology. The minimum gamma-ray luminosity is set at $L_{\gamma,\rm min} = 10^{39}$ erg s^{-1} because there are no reported gamma-ray-loud radio galaxies below this value. Here $\omega(F_\gamma[L_\gamma, z])$ is the detection efficiency of *Fermi* at the photon flux F_γ, which corresponds to the flux from a source with a gamma-ray luminosity L_γ at redshift z.

High-energy γ-rays ($\gtrsim$20 GeV) propagating through the universe are absorbed by the interaction with the extragalactic background light (EBL), also called the cosmic optical and infrared background (Salamon & Stecker 1998; Totani & Takeuchi 2002; Kneiske et al. 2004; Stecker et al. 2006; Mazin & Raue 2007; Raue & Mazin 2008; Franceschini et al. 2008; Razzaque et al. 2009; Gilmore et al. 2009; Finke et al. 2010; Kneiske & Dole 2010). Note that $\tau_{\gamma,\gamma}(\epsilon, z)$ is the optical depth of this background radiation. In this study, we adopt the model of Finke et al. (2010) for EBL and $\tau_{\gamma,\gamma}$.

The gamma-ray absorption creates electron–positron pairs. These pairs scatter the cosmic microwave background radiation to cause a secondary emission component (the so-called cascade emission) in addition to the absorbed primary emission (Aharonian et al. 1994; Wang et al. 2001; Dai et al. 2002; Razzaque et al. 2004; Ando 2004; Murase et al. 2007; Kneiske & Mannheim 2008; Inoue & Totani 2009; Venters 2010). We take into account the first generation of the cascade emission following the formulations in Kneiske & Mannheim (2008). In the following result, the cascade emission has a small effect on the EGRB flux. Hence, the other generations of the cascade emission do not have serious effects on our conclusion in this study.

Figure 3 shows the νI_ν EGRB spectrum in the unit of MeV^2 cm^{-2} s^{-1} MeV^{-1} sr^{-1} predicted by our GLFs. The intrinsic (the spectrum without the EBL absorption effect), absorbed, and cascade components of the EGRB spectrum and the total EGRB spectrum (absorbed+cascade) are shown. The data of *HEAO-1* (Gruber et al. 1999), *Swift* Burst Alert Telescope (BAT; Ajello et al. 2008), *SMM* (Watanabe et al. 1997), COMPTEL (Kappadath et al. 1996), and *Fermi*-LAT (Abdo et al. 2010e) are also shown. As seen in the figure, the cascade emission does not significantly contribute to the EGRB spectrum.

The expected EGRB photon flux above 100 MeV from gamma-ray-loud radio galaxy populations is 0.26×10^{-5} photons cm^{-2} s^{-1} sr^{-1}. As the unresolved *Fermi* EGRB flux above 100 MeV is 1.03×10^{-5} photons cm^{-2} s^{-1} sr^{-1} (Abdo et al. 2010e), the gamma-ray-loud radio galaxies explain $\sim$25% of the unresolved EGRB flux. For comparison, recent analysis of *Fermi* blazars showed that blazars explain $\sim$22% of the unresolved EGRB (Abdo et al. 2010f). Therefore, radio-loud AGN populations can explain $\sim$47% of the EGRB.

To avoid instrument dependence, we also evaluate the total EGRB photon flux (i.e., resolved + unresolved) from gamma-ray-loud radio galaxies. The contribution to total EGRB is 0.27×10^{-5} photons cm^{-2} s^{-1} sr^{-1} and this corresponds to $\sim$19% of total the *Fermi* EGRB flux, which is 1.42×10^{-5} photons cm^{-2} s^{-1} sr^{-1} (Abdo et al. 2010e).

Figure 3 also shows that gamma-ray-loud radio galaxies would also significantly contribute to the MeV EGRB at $>$1 MeV. Although it has been suggested that this is caused by radio-quiet AGNs (Inoue et al. 2008), MeV blazars (Ajello et al. 2009), and MeV DM annihilation (e.g., Ahn & Komatsu 2005a), it is still uncertain because of the lack of observational evidence. As shown in this study, gamma-ray-loud radio galaxies would also be a candidate for the origin of the MeV background. This situation will be solved by future X-ray and MeV gamma-ray experiments such as the *Astro-H*[3] mission (Takahashi et al. 2010) and the DUAL gamma-ray mission (Boggs et al. 2010), respectively.

We now examine the uncertainties in the model prediction. Since the normalization of the GLF is determined from ten samples, there is a statistical uncertainty of 32% in its normalization of the EGRB at 68% confidence level. The correlation of the radio and gamma-ray luminosities also has uncertainties in their slope and normalization as in Section 3.1. By taking into account those uncertainties, the fraction of gamma-ray-loud radio galaxies in the unresolved EGRB varies from $\sim$10% to $\sim$63%. Furthermore, as discussed by Stecker & Venters (2010), the energy dependence of source-confusion effects would alter the EGRB spectrum below $\sim$1 GeV. However, the angular resolution also depends on the position of the source in the field of view (Atwood et al. 2009). Further careful evaluation is required to discuss the source-confusion effects.

5. DISCUSSION

5.1. Fraction of Gamma-ray-loud Radio Galaxies

Since a jet is brighter to observers with a smaller viewing angle from the jet axis because of the beaming effect, the fraction of gamma-ray-loud radio galaxies κ would be related to the viewing angle. It is believed that radio galaxies have bipolar

[3] *Astro-H*: http://astro-h.isas.jaxa.jp/index.html.en

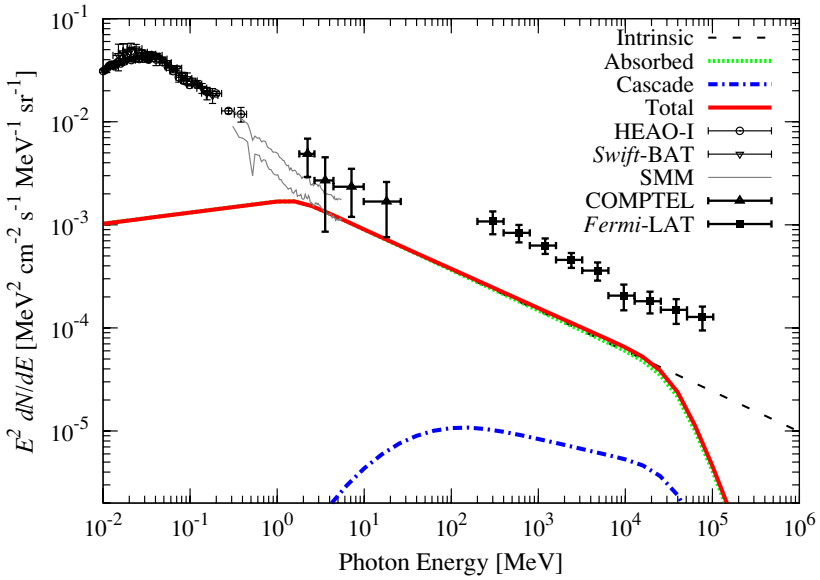

Figure 3. EGRB spectrum from gamma-ray-loud radio galaxies in the unit of $\mathrm{MeV^2\,cm^{-2}\,s^{-1}\,MeV^{-1}\,sr^{-1}}$. Dashed, dotted, dot-dashed, and solid curves show the intrinsic spectrum (no absorption), and the absorbed, cascade, and total (absorbed+cascade) EGRB spectrum, respectively. The observed data of *HEAO-1* (Gruber et al. 1999), *Swift*-BAT (Ajello et al. 2008), *SMM* (Watanabe et al. 1997), COMPTEL (Kappadath et al. 1996), and *Fermi*-LAT (Abdo et al. 2010e) are also shown by the symbols indicated in the figure.

(A color version of this figure is available in the online journal.)

jets (Urry & Padovani 1995). The fraction of radio galaxies with viewing angle $<\theta$ is given as $\kappa = (1 - \cos\theta)$. In this study, the fraction of gamma-ray-loud radio galaxies is derived as $\kappa = 0.081$, as discussed in Section 3.3. Then, the expected θ is $\lesssim 24^\circ$. The viewing angle of NGC 1275, M 87, and Cen A is derived as 25°, 10°, and 30° by SED fitting (Abdo et al. 2009b, 2009c, 2010c), respectively. Therefore, our estimation is consistent with the observed results.

Here, beaming factor δ is defined as $\Gamma^{-1}(1-\beta\cos\theta)^{-1}$, where Γ is the bulk Lorentz factor of the jet and $\beta = \sqrt{1-1/\Gamma^2}$. If $\Gamma \sim 10$, which is typical for blazars, δ becomes $\sim$1 with $\theta = 24^\circ$. This value means no significant beaming effect because the observed luminosity is δ^4 times brighter than that in the jet rest frame. On the other hand, if $2 \lesssim \Gamma \lesssim 4$, δ becomes greater than 2 with $\theta = 24^\circ$ (i.e., the beaming effect becomes important). Ghisellini et al. (2005) proposed the spine and layer jet emission model, in which the jet is composed of a slow jet layer and a fast jet spine. The difference of Γ between blazars and gamma-ray-loud radio galaxies would be interpreted using a structured jet emission model.

We note that κ depends on α_r, as in Section 3.2. By changing α_r by 0.1 (i.e., to 0.7 or 0.9), κ and θ change by a factor of 1.4 and 1.2, respectively. Thus, even if we change α_r, the beaming effect is not effective if $\Gamma \sim 10$ but with a lower Γ value, $2 \lesssim \Gamma \lesssim 4$.

5.2. Uncertainty in the Spectral Modeling

As pointed out in Section 2, there are uncertainties in SED modeling because of small samples, such as the photon index (Γ) and the break photon energy ($\epsilon_{\rm br}$). In the case of blazars, Stecker & Salamon (1996) and Pavlidou & Venters (2008) calculated the blazar EGRB spectrum including the distribution of the photon index by assuming Gaussian distributions even with $\sim$50 samples. We performed the Kolomogorov–Smirnov test to determine the goodness of fit of the Gaussian distribution to our sample, and to check whether the method of Stecker & Salamon (1996) and Pavlidou & Venters (2008) is applicable to our sample. The chance probability is 12%. This means that the Gaussian distribution does not agree with the data. To investigate the distribution of the photon index, more samples would be required.

We evaluate the uncertainties in SED models by using various SEDs. Figure 4 shows the total EGRB spectrum (absorbed + cascade) from the gamma-ray-loud radio galaxies with various photon index and break energy parameters. The contribution to the unresolved *Fermi* EGRB photon flux above 100 MeV becomes 25.4%, 25.4%, and 23.8% for $\Gamma = 2.39$, 2.11, and 2.67, respectively. In the case of $\Gamma = 2.11$, the contribution to the EGRB flux above 10 GeV becomes significant. For the MeV background below 10 MeV, the position of the break energy and the photon index is crucial to determine the contribution of the gamma-ray-loud radio galaxies. As shown in Figure 4, higher break energy and softer photon index result in a smaller contribution to the MeV background radiation. To enable further discussion on the SED modeling, the multiwavelength spectral analysis of all GeV-observed gamma-ray-loud radio galaxies is required.

5.3. Flaring Activity

It is well known that blazars are variable sources in gamma rays (see, e.g., Abdo et al. 2009a, 2010d). If gamma-ray-loud radio galaxies are the misaligned populations of blazars, they will also be variable sources. Kataoka et al. (2010) have recently reported that NGC 1275 showed a factor of $\sim$2 variation in the gamma-ray flux. For other gamma-ray-loud radio galaxies, such a significant variation has not been observed yet (Abdo et al. 2010b). Currently, therefore, it is not straightforward to model the variability of radio galaxies. In this paper, we used the time-averaged gamma-ray flux of gamma-ray-loud radio galaxies in the *Fermi* catalog, which is the mean of the *Fermi* 1 yr observation. More observational information (e.g., frequency) is required to model the gamma-ray variability of radio galaxies. Further long-term *Fermi* observation will be useful, and future observation by ground-based imaging atmospheric Cherenkov

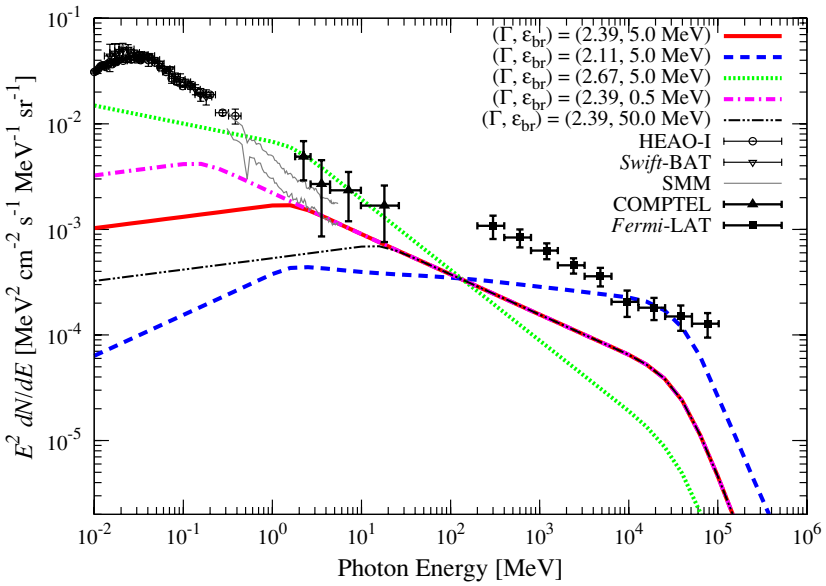

Figure 4. Gamma-ray-loud radio galaxy EGRB spectra in the unit of (MeV^2 cm^{-2} s^{-1} MeV^{-1} sr^{-1}) for various SED parameters, Γ and $\epsilon_{\rm br}$. The curves shown are the total EGRB spectrum (absorbed + cascade). Solid, dashed, dotted, dot-dashed, and double-dotted dashes curves correspond to the EGRB spectrum with (Γ, $\epsilon_{\rm br}$) = (2.39, 5.0 MeV), (2.11, 5.0 MeV), (2.67, 5.0 MeV), (2.39, 0.5 MeV), and (2.39, 50.0 MeV), respectively. The observed data shown here are the same as in Figure 3.

(A color version of this figure is available in the online journal.)

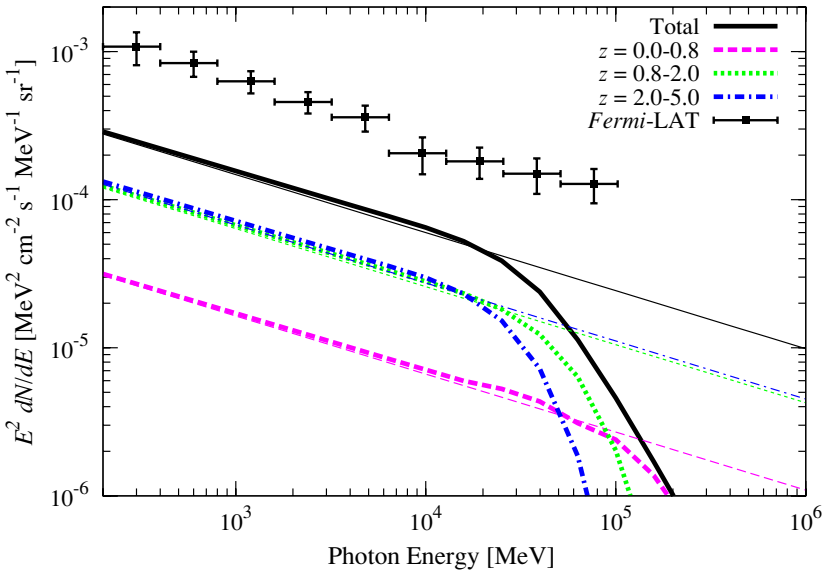

Figure 5. Gamma-ray-loud radio galaxy EGRB spectra in the unit of (MeV^2 cm^{-2} s^{-1} MeV^{-1} sr^{-1}) at each redshift bin. Solid, dashed, dotted, and dot-dashed curves show the EGRB spectrum at z = 0.0–5.0, z = 0.0–0.8, z = 0.8–2.0, and z = 2.0–5.0, respectively. The thin and thick curves correspond to the intrinsic spectrum (not absorbed) and the total spectrum (absorbed + cascade), respectively. The observed data of *Fermi*-LAT (Abdo et al. 2010e) are also shown.

(A color version of this figure is available in the online journal.)

telescope at the Cherenkov Telescope Array (CTA)[4] would be key to understanding short-period variabilities.

5.4. Origin of the GeV EGRB

In this study, we find that the contribution of gamma-ray-loud radio galaxies to the unresolved EGRB above 100 MeV is ∼25%. Abdo et al. (2010f) recently showed that unresolved blazars can explain only ∼22% of the unresolved EGRB by analyzing the 1 yr catalog of the *Fermi* blazars. Therefore, the origin of the remaining ∼53% of the EGRB is still missing.

Various gamma-ray emitting extragalactic sources have also been discussed as the GeV EGRB origin, as mentioned in the fourth paragraph of Section 1. Figure 5 shows the gamma-ray-loud radio galaxy EGRB spectra at each redshift bin. Because of the EBL, the spectrum above 30 GeV shows the absorbed signature. Here, the cosmological sources, such as star formation history and AGN activity, have evolution peaks at z = 1–2 (see, e.g., Hopkins & Beacom 2006; Ueda et al. 2003). This means that the gamma rays from extragalactic sources (e.g., galaxies and AGNs) will experience the EBL absorption. However, as shown in Figure 5, *Fermi* EGRB spectrum does not show such an absorbed signature. This might suggest that nearby gamma-ray-emitting sources or sources with very hard gamma ray spectra

[4] CTA: http://www.cta-observatory.org/

would be the dominant population of EGRB above 10 GeV. To address this issue, we should await the EGRB information above 100 GeV from future observations such as those done by *Fermi*. CTA would also be able to see the EGRB at a much higher energy band. We also need to examine the EBL models at high redshifts. It is expected that CTA will see blazars up to $z \sim 1.2$ at the very high energy band >30 GeV (Inoue et al. 2010). Therefore, *Fermi* and CTA will be key to understanding the origin of the EGRB.

5.5. Implication for the AGN Unification Scenario

The AGN unification scenario explains various properties of AGNs in terms of the viewing angle (Urry & Padovani 1995). In the scheme of the AGN jet unification scenario, FRI and FRII galaxies are thought to be misaligned populations of BL Lac objects and FSRQs, respectively.

From Table 1, the mean photon indices of FRIs and FRIIs are 2.27 and 2.58, respectively. Therefore, the FRI population tends to have harder spectra than the FRII population, as shown by Abdo et al. (2010b). This trend is also the same as that between BL Lac objects and FSRQs (Abdo et al. 2010g). This result would support the observation that FRIs and FRIIs are the misaligned populations of BL Lac objects and FSRQs.

It is also important to compare the cosmological evolution of blazars and radio galaxies based on the recent *Fermi* data. Although a theoretical blazar GLF model (Inoue & Totani 2009) is briefly compared with the Fermi blazar data (Inoue et al. 2010, 2011; Inoue & Totani 2011), a comparison of the redshift space has not yet been performed. This is because redshifts of about half of the BL Lac samples have not yet been determined (Abdo et al. 2010g).

Using the blazar sequence, Inoue & Totani (2009) treated blazars as a single population (Fossati et al. 1998; Kubo et al. 1998). Blazar GLF models that divide FSRQs and BL Lac objects are required to interpret the unification scenario (Dermer 2007). In addition, since our model does not treat FRI and FRII separately because of small samples, GLF models of gamma-ray-loud radio galaxies dividing these two populations are also required.

Therefore, redshift information for all blazars and more gamma-ray-loud radio galaxy data would be required to make a comparison between the cosmological evolution of blazars and radio galaxies.

6. CONCLUSION

In this paper, we studied the contribution of gamma-ray-loud radio galaxies to the EGRB by constructing their GLFs. First, we explored the correlation between the radio and gamma-ray luminosities of gamma-ray-loud radio galaxies, which have recently been reported by *Fermi* (Abdo et al. 2010b, 2010g). Through a partial correlation analysis, we found that there is a correlation $L_\gamma \propto L_{5\,\mathrm{GHz}}^{1.16\pm0.02}$ where L_γ is the 0.1–10 GeV gamma-ray luminosity and $L_{5\,\mathrm{GHz}}$ is the radio luminosity at 5 GHz. This slope index is similar to that of blazars.

Based on this correlation, we defined the GLF of gamma-ray-loud radio galaxies using the RLF of radio galaxies. We normalized the GLF to fit the cumulative flux distribution of *Fermi* samples by using the *Fermi* detection efficiency (Abdo et al. 2010f). We then predicted the contribution of gamma-ray-loud radio galaxies to the MeV and GeV EGRB. The absorption by the EBL and the reprocessed cascade emission are also taken into account. We found that gamma-ray-loud radio galaxies will explain ~25% of the EGRB flux above 100 MeV and also make a significant contribution to the 1–30 MeV EGRB. Since blazars explain ~22% of the EGRB, we are able to explain ~47% of the EGRB with blazars and gamma-ray-loud radio galaxies.

We also gave an interpretation on the origin of the EGRB above 10 GeV from the point of view of the EBL absorption effect. Since the EBL absorption signature still does not appear in the EGRB spectrum, the origin would be nearby sources or sources with hard gamma-ray spectra. We await EGRB data at a higher energy band to explore this issue.

The author thanks the hospitality of the Max Planck Institute for Physics at Munich where this work took place. The author also thanks M. Hayashida, D. Paneque, and H. Takami for discussion, and the anonymous referee for his/her constructive suggestions. This work was supported by the Grant-in-Aid for the Global COE Program "The Next Generation of Physics, Spun from Universality and Emergence" and the Grant-in-Aid for Scientific Research (19047003, 19740099) from the Ministry of Education, Culture, Sports, Science and Technology (MEXT) of Japan. The author also acknowledges support by the Research Fellowship of the Japan Society for the Promotion of Science (JSPS).

APPENDIX

PARTIAL CORRELATION ANALYSIS

To study the correlation between luminosities at different wavelengths, we use luminosities directly. However, the correlation in luminosity space is distorted by redshift if samples are flux-limited. This will result in a spurious correlation. Therefore, we need to test the correlation excluding the redshift dependence. Partial correlation analysis is used as the analyzing method for such a condition (see Padovani 1992 for details). The partial correlation analysis method is as follows.

We have parameter sets of $(x_i, y_i, z_i), i = 1, 2, \ldots, N$. Let X_i be the rank of x_i among the other x, Y_i be the rank of y_i among the other y, and Z_i be the rank of z_i among the other z. The Spearman rank–order correlation coefficient between x and y is defined to be the linear correlation coefficient of the ranks as

$$r_{xy} = \frac{\Sigma_{i=1}^{N}(X_i - \overline{X})(Y_i - \overline{Y})}{\sqrt{\Sigma_{i=1}^{N}(X_i - \overline{X})^2}\sqrt{\Sigma_{i=1}^{N}(Y_i - \overline{Y})^2}}, \quad \text{(A1)}$$

where $\overline{X}$ and $\overline{Y}$ are the mean of the X and the Y, respectively (see Press et al. 1992 for details). The correlation coefficients between x and z, and y and z, are also given in the same way. Then, the correlation coefficient between x and y excluding the dependence on the third parameter of z is evaluated as

$$r_{xy,z} = \frac{r_{xy} - r_{xz}r_{yz}}{\sqrt{1 - r_{xz}^2}\sqrt{1 - r_{yz}^2}}, \quad \text{(A2)}$$

where r_{xz} and r_{yz} are the correlation coefficients between x and z and between y and z, respectively (Kendall & Stuart 1979).

REFERENCES

Abdo, A. A., et al. 2009a, ApJ, 699, 817
Abdo, A. A., et al. 2009b, ApJ, 699, 31
Abdo, A. A., et al. 2009c, ApJ, 707, 55
Abdo, A. A., et al. 2010a, ApJS, 188, 405
Abdo, A. A., et al. 2010b, ApJ, 720, 912

Abdo, A. A., et al. 2010c, ApJ, 719, 1433
Abdo, A. A., et al. 2010d, ApJ, 722, 520
Abdo, A. A., et al. 2010e, Phys. Rev. Lett., 104, 101101
Abdo, A. A., et al. 2010f, ApJ, 720, 435
Abdo, A. A., et al. 2010g, ApJ, 715, 429
Aharonian, F. A., Coppi, P. S., & Voelk, H. J. 1994, ApJ, 423, L5
Ahn, E., Bertone, G., Merritt, D., & Zhang, P. 2007, Phys. Rev. D, 76, 023517
Ahn, K., & Komatsu, E. 2005a, Phys. Rev. D, 71, 021303
Ahn, K., & Komatsu, E. 2005b, Phys. Rev. D, 72, 061301
Ahn, K., Komatsu, E., & Höflich, P. 2005, Phys. Rev. D, 71, 121301
Ajello, M., et al. 2008, ApJ, 689, 666
Ajello, M., et al. 2009, ApJ, 699, 603
Ando, S. 2004, MNRAS, 354, 414
Ando, S. 2009, Phys. Rev. D, 80, 023520
Ando, S., & Komatsu, E. 2006, Phys. Rev. D, 73, 023521
Ando, S., Komatsu, E., Narumoto, T., & Totani, T. 2007, Phys. Rev. D, 75, 063519
Atwood, W. B., et al. 2009, ApJ, 697, 1071
Baum, S. A., Heckman, T. M., Bridle, A., van Breugel, W. J. M., & Miley, G. K. 1988, ApJS, 68, 643
Bennett, A. S. 1962, MNRAS, 125, 75
Bergström, L. 2000, Rep. Prog. Phys., 63, 793
Bhattacharya, D., & Sreekumar, P. 2009, Res. Astron. Astrophys., 9, 509
Bhattacharya, D., Sreekumar, P., & Mukherjee, R. 2009, Res. Astron. Astrophys., 9, 85
Boggs, S., et al. 2010, arXiv:1006.2102v1
Boldt, E. 1987, Phys. Rep., 146, 215
Burgess, A. M., & Hunstead, R. W. 2006a, AJ, 131, 100
Burgess, A. M., & Hunstead, R. W. 2006b, AJ, 131, 114
Burns, J. O., Feigelson, E. D., & Schreier, E. J. 1983, ApJ, 273, 128
Chiang, J., Fichtel, C. E., von Montigny, C., Nolan, P. L., & Petrosian, V. 1995, ApJ, 452, 156
Chiang, J., & Mukherjee, R. 1998, ApJ, 496, 752
Clayton, D. D., & Ward, R. A. 1975, ApJ, 198, 241
Dai, Z. G., Zhang, B., Gou, L. J., Mészáros, P., & Waxman, E. 2002, ApJ, 580, L7
Dermer, C. D. 2007, ApJ, 659, 958
Dondi, L., & Ghisellini, G. 1995, MNRAS, 273, 583
Dunlop, J. S., & Peacock, J. A. 1990, MNRAS, 247, 19
Ekers, R. D., et al. 1989, MNRAS, 236, 737
Fabian, A. C., & Barcons, X. 1992, ARA&A, 30, 429
Fanaroff, B. L., & Riley, J. M. 1974, MNRAS, 167, 31P
Faucher-Giguère, C., & Loeb, A. 2010, J. Cosmol. Astropart. Phys., JCAP01(2010)005
Fichtel, C. E., Simpson, G. A., & Thompson, D. J. 1978, ApJ, 222, 833
Fields, B. D., Pavlidou, V., & Prodanović, T. 2010, ApJ, 722, L199
Finke, J. D., Razzaque, S., & Dermer, C. D. 2010, ApJ, 712, 238
Fossati, G., Maraschi, L., Celotti, A., Comastri, A., & Ghisellini, G. 1998, MNRAS, 299, 433
Franceschini, A., Rodighiero, G., & Vaccari, M. 2008, A&A, 487, 837
Gabici, S., & Blasi, P. 2003, Astropart. Phys., 19, 679
Ghirlanda, G., Ghisellini, G., Tavecchio, F., & Foschini, L. 2010, MNRAS, 407, 791
Ghirlanda, G., Ghisellini, G., Tavecchio, F., Foschini, L., & Bonnoli, G. 2011, MNRAS, tmp, 418
Ghisellini, G., Tavecchio, F., & Chiaberge, M. 2005, A&A, 432, 401
Gilli, R., Comastri, A., & Hasinger, G. 2007, A&A, 463, 79
Gilmore, R. C., Madau, P., Primack, J. R., Somerville, R. S., & Haardt, F. 2009, MNRAS, 399, 1694
Giommi, P., Colafrancesco, S., Cavazzuti, E., Perri, M., & Pittori, C. 2006, A&A, 445, 843
Gruber, D. E., Matteson, J. L., Peterson, L. E., & Jung, G. V. 1999, ApJ, 520, 124
Hartman, R. C., et al. 1999, ApJS, 123, 79
Hasinger, G., Miyaji, T., & Schmidt, M. 2005, A&A, 441, 417
Hopkins, A. M., & Beacom, J. F. 2006, ApJ, 651, 142
Horiuchi, S., & Ando, S. 2006, Phys. Rev. D, 74, 103504
Horiuchi, S., & Beacom, J. F. 2010, ApJ, 723, 329
Inoue, Y., Inoue, S., Kobayashi, M. A. R., Totani, T., Kataoka, J., & Sato, R. 2011, MNRAS, 411, 464
Inoue, Y., & Totani, T. 2009, ApJ, 702, 523
Inoue, Y., & Totani, T. 2011, ApJ, 728, 73
Inoue, Y., Totani, T., & Mori, M. 2010, PASJ, 62, 1005
Inoue, Y., Totani, T., & Ueda, Y. 2008, ApJ, 672, L5
Jones, P. A., & McAdam, W. B. 1992, ApJS, 80, 137
Jungman, G., Kamionkowski, M., & Griest, K. 1996, Phys. Rep., 267, 195
Kappadath, S. C., et al. 1996, A&AS, 120, C619
Kataoka, J., et al. 2010, ApJ, 715, 554
Kawasaki, M., Kohri, K., & Nakayama, K. 2009, Phys. Rev. D, 80, 023517
Kendall, M., & Stuart, A. (ed.) 1979, The Advanced Theory of Statistics. Vol. 2: Inference and Relationship (New York: Oxford Univ. Press)
Keshet, U., Waxman, E., Loeb, A., Springel, V., & Hernquist, L. 2003, ApJ, 585, 128
Kneiske, T. M., Bretz, T., Mannheim, K., & Hartmann, D. H. 2004, A&A, 413, 807
Kneiske, T. M., & Dole, H. 2010, A&A, 515, A19
Kneiske, T. M., & Mannheim, K. 2008, A&A, 479, 41
Kubo, H., Takahashi, T., Madejski, G., Tashiro, M., Makino, F., Inoue, S., & Takahara, F. 1998, ApJ, 504, 693
Laing, R. A., Riley, J. M., & Longair, M. S. 1983, MNRAS, 204, 151
Linfield, R., & Perley, R. 1984, ApJ, 279, 60
Loeb, A., & Waxman, E. 2000, Nature, 405, 156
Makiya, R., Totani, T., & Kobayashi, M. A. R. 2011, ApJ, 728, 158
Massaro, F., & Ajello, M. 2011, ApJ, 729, L12
Mazin, D., & Raue, M. 2007, A&A, 471, 439
Miniati, F. 2002, MNRAS, 337, 199
Morganti, R., Killeen, N. E. B., & Tadhunter, C. N. 1993, MNRAS, 263, 1023
Mücke, A., & Pohl, M. 2000, MNRAS, 312, 177
Muecke, A., et al. 1997, A&A, 320, 33
Mukherjee, R., & Chiang, J. 1999, Astropart. Phys., 11, 213
Murase, K., Asano, K., & Nagataki, S. 2007, ApJ, 671, 1886
Narumoto, T., & Totani, T. 2006, ApJ, 643, 81
Oda, T., Totani, T., & Nagashima, M. 2005, ApJ, 633, L65
Padovani, P. 1992, A&A, 256, 399
Padovani, P., Ghisellini, G., Fabian, A. C., & Celotti, A. 1993, MNRAS, 260, L21
Pavlidou, V., & Fields, B. D. 2002, ApJ, 575, L5
Pavlidou, V., & Venters, T. M. 2008, ApJ, 673, 114
Press, W. H., Teukolsky, S. A., Vetterling, W. T., & Flannery, B. P. (ed.) 1992, Numerical Recipes in C: The Art of Scientific Computing (New York: Cambridge Univ. Press)
Raue, M., & Mazin, D. 2008, Int. J. Mod. Phys. D, 17, 1515
Razzaque, S., Dermer, C. D., & Finke, J. D. 2009, ApJ, 697, 483
Razzaque, S., Mészáros, P., & Zhang, B. 2004, ApJ, 613, 1072
Rybicki, G. B., & Lightman, A. P. (ed.) 1979, Radiative Processes in Astrophysics (Wiley: New York)
Saikia, D. J., Subrahmanya, C. R., Patnaik, A. R., Unger, S. W., Cornwell, T. J., Graham, D. A., & Prabhu, T. P. 1986, MNRAS, 219, 545
Salamon, M. H., & Stecker, F. W. 1994, ApJ, 430, L21
Salamon, M. H., & Stecker, F. W. 1998, ApJ, 493, 547
Siegal-Gaskins, J. M., Reesman, R., Pavlidou, V., Profumo, S., & Walker, T. P. 2010, arXiv:1011.5501v1
Spinrad, H., Marr, J., Aguilar, L., & Djorgovski, S. 1985, PASP, 97, 932
Sreekumar, P., et al. 1998, ApJ, 494, 523
Stawarz, Ł., Kneiske, T. M., & Kataoka, J. 2006, ApJ, 637, 693
Stecker, F. W., Malkan, M. A., & Scully, S. T. 2006, ApJ, 648, 774
Stecker, F. W., & Salamon, M. H. 1996, ApJ, 464, 600
Stecker, F. W., Salamon, M. H., & Malkan, M. A. 1993, ApJ, 410, L71
Stecker, F. W., & Venters, T. M. 2010, ApJ, submitted, arXiv:1012.3678v1
Strigari, L. E., Beacom, J. F., Walker, T. P., & Zhang, P. 2005, J. Cosmol. Astropart. Phys., JCAP04(2005)017
Strong, A. W., Moskalenko, I. V., & Reimer, O. 2004, ApJ, 613, 956
Takahashi, T., et al. 2010, Proc. SPIE, 7732, 77320Z
Thompson, D. J., & Fichtel, C. E. 1982, A&A, 109, 352
Thompson, T. A., Quataert, E., & Waxman, E. 2007, ApJ, 654, 219
Totani, T., & Kitayama, T. 2000, ApJ, 545, 572
Totani, T., & Takeuchi, T. T. 2002, ApJ, 570, 470
Ueda, Y., Akiyama, M., Ohta, K., & Miyaji, T. 2003, ApJ, 598, 886
Ullio, P., Bergström, L., Edsjö, J., & Lacey, C. 2002, Phys. Rev. D, 66, 123502
Unger, S. W., Booler, R. V., & Pedlar, A. 1984, MNRAS, 207, 679
Urry, C. M., & Padovani, P. 1995, PASP, 107, 803
Venters, T. M. 2010, ApJ, 710, 1530
Wang, X. Y., Dai, Z. G., & Lu, T. 2001, ApJ, 556, 1010
Watanabe, K., Hartmann, D. H., Leising, M. D., & The, L. 1999, ApJ, 516, 285
Watanabe, K., Hartmann, D. H., Leising, M. D., The, L., Share, G. H., & Kinzer, R. L. 1997, in AIP Conf. Ser. 410, Proc. Fourth Compton Symp., ed. C. D. Dermer, M. S. Strickman, & J. D. Kurfess (Melville, NY: AIP), 1223
Willott, C. J., Rawlings, S., Blundell, K. M., Lacy, M., & Eales, S. A. 2001, MNRAS, 322, 536
Zdziarski, A. A. 1996, MNRAS, 281, L9
Zhang, L., Cheng, K. S., & Fan, J. H. 2001, PASJ, 53, 207